Vol 18 No 7, July 2009
1674-1056/2009/18(07)/2801-05

Chinese Physics B

© 2009 Chin. Phys. Soc.
and IOP Publishing Ltd

A dual-loop Sagnac interferometer*

Ma Hai-Qiang(马海强)[a)b)], Zhao Jian-Ling(赵建领)[b)], and Wu Ling-An(吴令安)[b)†]

[a)] *School of Sciences, Beijing University of Posts and Telecommunications, Beijing* 100876, *China*

[b)] *Laboratory of Optical Physics, Institute of Physics, Chinese Academy of Sciences, Beijing* 100190, *China*

(Received 23 February 2009; revised manuscript received 17 March 2009)

A new type of all-fibre Sagnac interferometer composed of two loops is proposed and analysed in detail. It can be used with a very long transmission line while maintaining excellent performance characteristics due to the automatic compensation of any birefringence effects in the trunk fibre. Preliminary experiments at 1310 nm wavelength with a 70 km long trunk fibre demonstrated an interference visibility as high as 98%, indicating that this scheme has promising potential applications.

Keywords: Sagnac interferometer, polarization controller
PACC: 4250, 4225K

Among the various kinds of optical interferometers the Sagnac interferometer is not so well known and is not even mentioned in many standard optics texts. It was first proposed in 1913 by Sagnac as a ring resonator to search for the 'ether drift' relative to a rotating frame.[1] In recent years, however, it has attracted much attention on account of its application in gyroscopes and in other special fields of research. Its characteristic properties include exceptional stability, easy maintenance, and relatively simple construction and production. As an optical sensor it has reached a high degree of maturity and has been widely used, especially with fibre optics, for example in the high-voltage environment of the electric power industry.[2] Other applications include gain flattening of erbium-doped fibre amplifiers,[3] fibre Bragg grating sensors,[4] measurement of the chromatic dispersion of an optical fibre,[5] and multiwavelength and wavelength-switched fibre lasers.[6,7] At the same time, various modified Sagnac interferometers have been proposed which reveal good prospects for application.[8,9] The fibre Sagnac interferometer may also play an important role in the newly emerging field of quantum information science for quantum key distribution[10,11] and for generating polarization-entangled photon pairs.[12,13] However, it is necessary to correct for polarization scrambling due to environmentally dependent birefringence that is a source of noise and signal fading in fibre-optic gyros. We describe here a new type of all-fibre Sagnac interferometer composed of two loops which can automatically compensate for any birefringence effects in a trunk fibre between the loops, and thus has excellent performance characteristics.

The paper is structured as follows. First, a brief overview is given of a simple Sagnac interferometer based on a 3 dB power splitting 2×2 fibre coupler. The principle of the dual-loop all-fibre Sagnac interferometer is then described in detail by the Jones matrix analysis approach. Finally, the results of experiments to demonstrate the scheme are reported.

The basic form of a fibre Sagnac interferometer is shown in Fig.1.

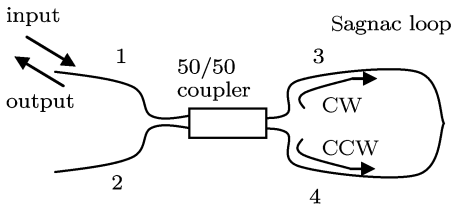


Fig.1. Schematic of a fibre Sagnac interferometer. 1, 2, 3 and 4: input and output ports; CW: clockwise; CCW: counterclockwise.

In the ideal case, light entering input port 1 is split by the 3 dB power splitting 2×2 fibre coupler into two counter-propagating waves of equal amplitude, with one part traveling clockwise (CW) through the loop and the other part counterclockwise (CCW). Consequently, when the two parts arrive at the coupler

*Project supported by the National Natural Science Foundation of China (Grant Nos 60578029, 10674174 and 10805006) and the National Program for Basic Research in China (Grant No 2006CB921100).

†E-mail: wula@aphy.iphy.ac.cn

again they have both traveled the same optical path distance so their relative phase difference can be stably maintained, and constructive interference occurs at the output port 1.[14] In general, this type of loop Sagnac interferometer is equivalent to an all-reflective mirror. The structure is very simple, but the loop fibre cannot be made very long as otherwise the delay between the times that two counter-propagating waves of the same polarization traverse a given point on the loop may be too long, and the change between the times of the fibre environment too great, leading to phase instabilities and degradation of the interference visibility. An improvement to this configuration, first implemented in a quantum key distribution system,[15] is to replace the fibre ring with a Faraday mirror, by means of which the birefringence effects can be automatically compensated for.

Figure 2 is a schematic of a dual-loop version of the fibre Sagnac interferometer based on two reversible polarizing beamsplitters. Its principle can be described as follows. A light wave of arbitrary polarization is injected through the circulator and then split at the 50/50% polarization-independent 2×2 coupler C to enter the first fibre loop. Two polarization controllers PC1 and PC2 are used to change the polarization directions of the output beams such that beam 1 in the upper arm is directed into the $\boldsymbol{p}$ polarization port of the 1×2 reversible polarizing beamsplitter PBS1, and beam 2 in the lower arm into the $\boldsymbol{s}$ polarization port. Both waves then travel through the trunk fibre and reach the second fibre loop which consists of another reversible 1×2 polarizing beamsplitter PBS2 and a $\lambda/2$ wave plate P. The polarization controller PC3 is used to correct the birefringence effects introduced by the trunk channel.[16] The $\boldsymbol{s}$ and $\boldsymbol{p}$ polarized incident waves are directed through the corresponding polarization output ports of PBS2, then P rotates the polarizations by 90° so that the incident light waves have exchanged their polarization states when they arrive at PBS2 for the second time. On traveling back through the trunk fibre and arriving once more at PBS1, the beam that originally passed through the upper arm will now take the lower arm since it has become $\boldsymbol{s}$ polarized, and vice versa for the other beam. After passage through PC1 and PC2 the polarizations of both arms revert to the same original state, so the two beams are able to interfere at the polarization-independent coupler C. Constructive interference will thus be registered at detector D_0 or D_1, depending on the relative phase changes encountered in the two loops. In essence, the interferometer can be thought of as a single extended Sagnac interferometer with its two counter-propagating waves going clockwise and anticlockwise through both first and second loops with the trunk line included.

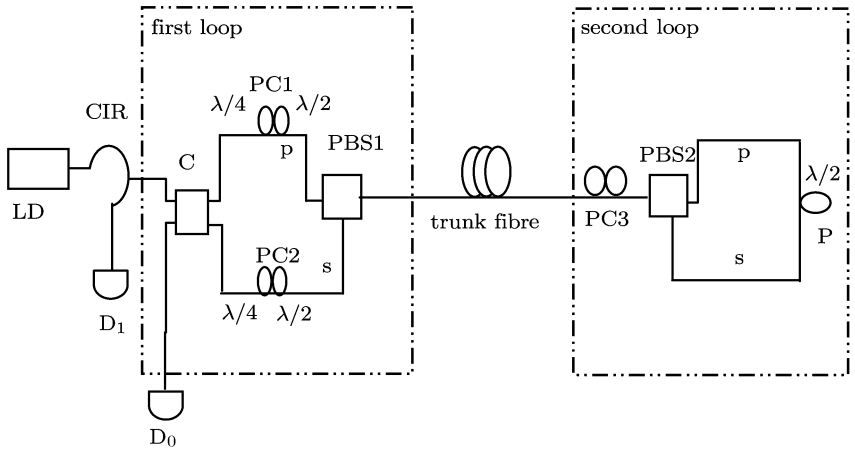


Fig.2. A dual-loop type Sagnac interferometer setup. LD: laser diode; CIR: circulator; D_0, D_1: power meters; C: 2×2 coupler; PC1, PC2, PC3: polarization controllers; P: $\lambda/2$ wave plate; PBS1, PBS2: reversible 1×2 polarizing beamsplitters with output polarization directions $\boldsymbol{p}$ and $\boldsymbol{s}$.

We now present a Jones matrix analysis of the dual-loop Sagnac interferometer. We assume that an input light wave, which is split and coupled into the two pigtails of the polarization-independent 2×2 coupler C is

initially in the linear polarization state:

$$\psi = \psi_{1,2} = \begin{bmatrix} E_x^0 \\ E_y^0 \end{bmatrix} = \frac{\sqrt{2}}{2} \begin{bmatrix} 1 \\ 1 \end{bmatrix}, \tag{1}$$

where ψ_1 and ψ_2 indicate the light waves entering the upper and lower arms, and x, y are the initial polarization directions of the electric field relative to the forward propagation direction $+\boldsymbol{z}$, respectively.

A polarization controller consists of two bat wing plates and is equivalent to a $\lambda/4$ and $\lambda/2$ waveplate in tandem. Their Jones transform matrices are, respectively,

$$T_{\lambda/4} = \begin{bmatrix} \cos\left(\frac{\pi}{4}\right) + \mathrm{i}\sin\left(\frac{\pi}{4}\right)\cos(2\beta) & \mathrm{i}\sin\left(\frac{\pi}{4}\right)\sin(2\beta) \\ \mathrm{i}\sin\left(\frac{\pi}{4}\right)\sin(2\beta) & \cos\left(\frac{\pi}{4}\right) - \mathrm{i}\sin\left(\frac{\pi}{4}\right)\cos(2\beta) \end{bmatrix} \tag{2}$$

and

$$T_{\lambda/2} = \begin{bmatrix} \cos\left(\frac{\pi}{2}\right) + \mathrm{i}\sin\left(\frac{\pi}{2}\right)\cos(2\gamma) & \mathrm{i}\sin\left(\frac{\pi}{2}\right)\sin(2\gamma) \\ \mathrm{i}\sin\left(\frac{\pi}{2}\right)\sin(2\gamma) & \cos\left(\frac{\pi}{2}\right) - \mathrm{i}\sin\left(\frac{\pi}{2}\right)\cos(2\gamma) \end{bmatrix}, \tag{3}$$

where β and γ are the angles between the fast axes in the $\lambda/4$ and $\lambda/2$ plates and the x axis, respectively, with the $+\boldsymbol{z}$ axis as the direction of light propagation, and the reference system is right-handed.

Beam ψ_1 is rotated by PC1 in the upper arm to the $\boldsymbol{p}$ polarized state ψ_1' before entering the input port of PBS1:

$$\psi_1' = \vec{T}_{\mathrm{PC1}} \cdot \psi_1 = \frac{\sqrt{2}}{2}(1 - \mathrm{i}) \begin{bmatrix} 0 \\ 1 \end{bmatrix}. \tag{4}$$

Similarly, ψ_2 passes through PC2 in the lower arm and becomes the $\boldsymbol{s}$ polarized state ψ_2' (here the vector relation $\boldsymbol{z} = \boldsymbol{p} \times \boldsymbol{s}$ is used, where $\boldsymbol{p}$ and $\boldsymbol{s}$ are the two input polarization directions of PBS1):

$$\psi_2' = \vec{T}_{\mathrm{PC2}} \cdot \psi_2 = \frac{\sqrt{2}}{2}(1 - \mathrm{i}) \begin{bmatrix} 1 \\ 0 \end{bmatrix}. \tag{5}$$

For convenience we adjust β and γ such that

$$\begin{aligned} \vec{T}_{\mathrm{PC1}} &= T_{\mathrm{PC1}\lambda/2} \cdot T_{\mathrm{PC1}\lambda/4} \\ &= \frac{\sqrt{2}}{2}\mathrm{i} \begin{bmatrix} 1 & -1 \\ -1 & -1 \end{bmatrix} \cdot \frac{\sqrt{2}}{2} \begin{bmatrix} 1 & \mathrm{i} \\ \mathrm{i} & 1 \end{bmatrix} \end{aligned} \tag{6}$$

and

$$\begin{aligned} \vec{T}_{\mathrm{PC2}} &= T_{\mathrm{PC2}\lambda/2} \cdot T_{\mathrm{PC2}\lambda/4} \\ &= \frac{\sqrt{2}}{2}\mathrm{i} \begin{bmatrix} -1 & -1 \\ -1 & 1 \end{bmatrix} \cdot \frac{\sqrt{2}}{2} \begin{bmatrix} 1 & \mathrm{i} \\ \mathrm{i} & 1 \end{bmatrix} \end{aligned} \tag{7}$$

are the forward transmission matrices for the polarization controllers PC1 and PC2, respectively. The two orthogonally polarized beams ψ_1' and ψ_2' pass through PBS1 and after propagating through the trunk fibre are directed through the corresponding polarization output ports of PBS2 by adjusting PC3. Then the half-wave plate P rotates the polarizations by 90° so that waves ψ_1' and ψ_2' have exchanged their polarization states when they arrive at PBS2 for the second time. The forward and backward Jones transform matrices for P can be written, respectively, as follows:

$$\vec{T}_{\mathrm{P}} = \mathrm{i} \begin{bmatrix} 0 & 1 \\ 1 & 0 \end{bmatrix}, \tag{8}$$

$$\vec{T}_{\mathrm{P}} = \mathrm{i} \begin{bmatrix} 0 & -1 \\ -1 & 0 \end{bmatrix}. \tag{9}$$

After passing through PC3, ψ_1 and ψ_2 become, respectively:

$$\begin{aligned} \psi_1'' = \vec{T}_{\mathrm{P}} \cdot \psi_1' &= \mathrm{i} \begin{bmatrix} 0 & 1 \\ 1 & 0 \end{bmatrix} \cdot \frac{\sqrt{2}}{2}(1 - \mathrm{i}) \begin{bmatrix} 0 \\ 1 \end{bmatrix} \\ &= \frac{\sqrt{2}}{2}\mathrm{i}(1 - \mathrm{i}) \begin{bmatrix} 1 \\ 0 \end{bmatrix} \end{aligned} \tag{10}$$

and

$$\psi_2'' = \overleftarrow{T}_{\rm P} \cdot \psi_2' = {\rm i} \begin{bmatrix} 0 & -1 \\ -1 & 0 \end{bmatrix} \cdot \frac{\sqrt{2}}{2}(1-{\rm i}) \begin{bmatrix} 1 \\ 0 \end{bmatrix} = -\frac{\sqrt{2}}{2}\,{\rm i}(1-{\rm i}) \begin{bmatrix} 0 \\ 1 \end{bmatrix}. \tag{11}$$

They then re-enter PBS2 to propagate back along the trunk fibre and re-enter PBS1. Now the wave ψ_1'' takes the lower arm, while ψ_2'' takes the upper arm. The reverse Jones transform matrices $T_{\rm PC2}$ and $T_{\rm PC1}$ in the lower and upper arms, respectively, are given by

$$\overleftarrow{T}_{\rm PC1} = T_{\rm PC1\lambda/4} \cdot T_{\rm PC1\lambda/2} = \frac{\sqrt{2}}{2} \begin{bmatrix} 1 & -{\rm i} \\ -{\rm i} & 1 \end{bmatrix} \cdot \frac{\sqrt{2}}{2}\,{\rm i} \begin{bmatrix} -1 & 1 \\ 1 & 1 \end{bmatrix} \tag{12}$$

and

$$\overleftarrow{T}_{\rm PC2} = T_{\rm PC2\lambda/4} \cdot T_{\rm PC2\lambda/2} = \frac{\sqrt{2}}{2} \begin{bmatrix} 1 & -{\rm i} \\ -{\rm i} & 1 \end{bmatrix} \cdot \frac{\sqrt{2}}{2}\,{\rm i} \begin{bmatrix} 1 & 1 \\ 1 & -1 \end{bmatrix}. \tag{13}$$

When the two waves arrive back at the coupler C, they are transformed to the states

$$\psi_1''' = \overleftarrow{T}_{\rm PC2} \cdot \psi_1'' = \frac{\rm i}{2} \begin{bmatrix} -1-{\rm i} & 1-{\rm i} \\ {\rm i}+1 & -{\rm i}+1 \end{bmatrix} \cdot \frac{\sqrt{2}}{2}\,{\rm i}(1-{\rm i}) \begin{bmatrix} 1 \\ 0 \end{bmatrix} = -\frac{\sqrt{2}}{2} \begin{bmatrix} -1 \\ 1 \end{bmatrix} \tag{14}$$

and

$$\psi_2''' = \overleftarrow{T}_{\rm PC1} \cdot \psi_2'' = \frac{\rm i}{2} \begin{bmatrix} 1-{\rm i} & 1+{\rm i} \\ -{\rm i}+1 & -{\rm i}-1 \end{bmatrix} \cdot \frac{-\sqrt{2}}{2}\,{\rm i}(1-{\rm i}) \begin{bmatrix} 0 \\ 1 \end{bmatrix} = -\frac{\sqrt{2}}{2} \begin{bmatrix} -1 \\ 1 \end{bmatrix}. \tag{15}$$

We thus see from equations (14) and (15) that the fields ψ_1''' and ψ_2''' have the same polarization and the same phase so that there is constructive interference registered at detector $\rm D_1$.

Another advantage of this dual Sagnac loop is the automatic compensation of any trunk fibre birefringence effects. The forward and backward Jones transform matrices for any birefringent trunk fibre can be expressed, respectively, as follows:

$$\overrightarrow{T}_{\rm trunk} = \begin{bmatrix} \cos\theta & -\sin\theta \\ \sin\theta & \cos\theta \end{bmatrix} \cdot \begin{bmatrix} \exp({\rm i}\,\theta_{\rm o}) & 0 \\ 0 & \exp({\rm i}\,\theta_{\rm e}) \end{bmatrix} \cdot \begin{bmatrix} \cos\theta & \sin\theta \\ -\sin\theta & \cos\theta \end{bmatrix}, \tag{16}$$

$$\overleftarrow{T}_{\rm trunk} = \begin{bmatrix} \cos\theta & \sin\theta \\ -\sin\theta & \cos\theta \end{bmatrix} \cdot \begin{bmatrix} \exp({\rm i}\,\theta_{\rm o}) & 0 \\ 0 & \exp({\rm i}\,\theta_{\rm e}) \end{bmatrix} \cdot \begin{bmatrix} \cos\theta & -\sin\theta \\ \sin\theta & \cos\theta \end{bmatrix}, \tag{17}$$

where $\exp({\rm i}\,\theta_{\rm o})$ and $\exp({\rm i}\,\theta_{\rm e})$ describe the phase and amplitude changes for propagation of the ordinary and extraordinary modes, θ is the rotation angle between the reference basis and the eigenmode basis of the fibre, and absorptive losses have been ignored.

When the clockwise propagating wave ψ_1' has completed a round trip and re-enters PBS1, the overall Jones matrix is:

$$T = \overleftarrow{T}_{\rm trunk} \cdot \overrightarrow{T}_{\rm P} \cdot \overrightarrow{T}_{\rm trunk} = \exp\{{\rm i}(\theta_{\rm o}+\theta_{\rm e})\}\boldsymbol{T}_{\rm P}. \tag{18}$$

A similar expression is obtained for the anticlockwise propagating wave, from which we see that there is no change in polarization, only a constant phase shift, regardless of the trunk fibre birefringence effects. Thus if a phase-sensitive sensor is placed in the second loop, with appropriate choice of arm lengths in the two loops, phase changes in the sensor may be detected at the detector outputs.

In order to quantify the performance of this dual-loop Sagnac interferometer, experiments were performed using the setup shown schematically in Fig.2. Linearly polarized light from a homemade 1.31 μm distributed feedback laser passes through the circulator, the first loop, a trunk line of single-mode SMF-28 optical fibre of different lengths, the second loop, and then back through the first loop to detectors $\rm D_0$ and

D_1 which are optical power meters. The laser output power was about 1.1 mW and the losses in each loop about 2dB. The visibility of the interferometer output is given by the expression

$$V = \frac{P_1 - P_0}{P_1 + P_0}, \tag{19}$$

where P_0 and P_1 are the powers measured at D_0 and D_1, respectively. Table 1 shows the results obtained for different lengths of the trunk fibre after accounting for scattered light introduced by Rayleigh backscattering in the fibre and back reflection from the connectors (10.3 nW). We see that the interference fringe visibility is greater than 98% for distances up to 70 km. This was maintained throughout two hours of observation time, showing the excellent capabilities of this dual-loop interferometer.

Table 1. Interference visibility measurements for the dual-loop Sagnac interferometer.
* Indicates the reading was taken on the nW setting of the power meter.

length/km	2.5	5	25	30	35	48	70
P_1/μW	483.38	330.57	15.82	7.399*	3.461*	0.479*	0.0169*
P_0/nW	510.50	500.00	80.00	20.30	15.10	4.01	0.16
visibility/%	99.6	99.6	99.6	99.4	99.1	98.1	98.1

In summary, we have designed a new dual-loop, all-fibre type of Sagnac interferometer and provided a detailed analysis of the optical field transformations. An excellent interference visibility of over 98% for trunk fibre lengths up to 70 km has been obtained in preliminary experiments, indicating promising applications for scientific research and industry, such as quantum cryptography, long-distance measurement, and environmental monitoring.

References

[1] Sagnac G 1913 *Comptes Rendus Acad. Sci.* **157** 708
Marlan O, Scully M and Zubairy S 1997 *Quantum Optics* (Cambridge: Cambridge University Press) p100

[2] Bohnert K, Gabus P, Kostovic J and Brandle H 2005 *Optics and Lasers in Engineering* **43** 511

[3] Li S, Chiang K S and Gambling W A 2001 *IEEE Photon. Technol. Lett.* **13** 942

[4] Chung S, Kim J, Yu B A and Lee B 2001 *IEEE Photon. Technol. Lett.* **13** 1343

[5] Abedin S K, Hyodo M and Onodera N 2000 *Opt. Lett.* **25** 299

[6] Dong X, Li S, Chiang K, Ng N M and Chu B C 2000 *Electron. Lett.* **36** 1609

[7] Yang S, Li Z, Dong X, Yuan S, Kai G and Zhao Q 2002 *IEEE Photon. Technol. Lett.* **14** 774

[8] Vakoc J B, Digonnet J M and Kino S G 2003 *Appl. Opt.* **42** 7132

[9] Fang X 1996 *J. Lightwave Tech.* **14** 2250

[10] Kumavor P D, Beal A C, Yelin S, Donkor E and Wang B C 2005 *J. Lightwave Tech.* **23** 268

[11] Nishioka T, Ishizuka H, Hasegawa T and Abe J 2002 *IEEE Photon. Technol. Lett.* **14** 576

[12] Li X, Paul L Voss, Sharping J E and Kumar P 2005 *Phys. Rev. Lett.* **94** 053601

[13] Shi B and Akihisa T 2004 *Phys. Rev.* A **69** 013803

[14] Birks A T and Morkel P 1988 *Appl. Opt.* **27** 3107

[15] Ribordy G, Gautier J D, Gisin N, Guinnard O and Zbinden H 2000 *J. Mod. Opt.* **47** 517

[16] Gobby C, Yuan L Z and Shields J A 2004 *Appl. Phys. Lett.* **84** 3762